

Combining Growcut And Temporal Correlation For IVUS Lumen Segmentation

Simone Balocco^{1,2}, Carlo Gatta^{1,2}, Francesco Ciompi^{1,2}, Oriol Pujol^{1,2}, Xavier Carrillo³, Josepa Mauri³, Petia Radeva^{1,2}

¹ Computer Vision Center, 08193 Bellaterra, Spain ² Dept. Matemàtica Aplicada i Anàlisi, Universitat de Barcelona, Gran Via 585, 08007 Barcelona, Spain ³ Hospital universitari Germans Trias i Pujol Badalona.

Abstract. The assessment of arterial luminal area, performed by IVUS analysis, is a clinical index used to evaluate the degree of coronary artery disease. In this paper we propose a novel approach to automatically segment the vessel lumen, which combines model-based temporal information extracted from successive frames of the sequence, with spatial classification using the Growcut algorithm. The performance of the method is evaluated by an *in vivo* experiment on 300 IVUS frames. The automatic and manual segmentation performances in general vessel and stent frames are comparable. The average segmentation error in vessel, stent and bifurcation frames are 0.17 ± 0.08 mm, 0.18 ± 0.07 mm and 0.31 ± 0.12 mm respectively.

1 Introduction

Atherosclerosis is a progressive disease affecting arterial blood vessels. The accurate assessment of luminal area is one of the most important guiding parameters during percutaneous intervention. It allows in fact to evaluate the local amount of stenosis, thus determining the degree of Coronary Artery Disease (CAD). The clinical inspection of coronary arteries is in general performed through Intravascular Ultrasound (IVUS) which is a catheter-based imaging technique providing real-time hi-resolution cross-sectional sequences. The IVUS sequence (pullback) can be represented as $I(x, y; t)$ where x and y are the spatial coordinates of the image (Figure 1), and t the frame number of a pullback.

Several automatic methods for segmentation the arterial lumen of IVUS images has been proposed so far. Recently a robust approach for lumen segmentation, based on the RF signal processing has been presented. [1]. This method requires dedicated hardware or a RF export device which is not commercially available and widespread in hospitals.

A second category of algorithms aims at segmenting the luminal contour using region growing techniques on the gray scale reconstructed images [1–4]. Those methods exploit probabilistic approaches based on active shape models. However, when blood and plaque present similar echogenicity, as in the case of Figure 1, the methods based on the local image statistics, become less robust and occasionally fail to identify the contour of the lumen. The main difficulty

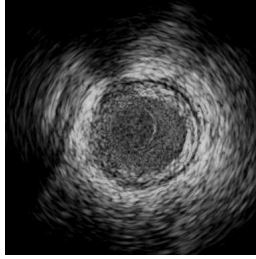


Fig. 1. IVUS image of a pathological patient artery. The plaque contour can hardly be defined on the left region because of the similar echogenicity with the blood.

lies in the impossibility to distinguish the changes in the statistical properties of the two contiguous areas. Such limitation was partially solved by several authors [5–7] who proposed the contemporaneous segmentation of successive frames of the pullback in order to improve the robustness of the method. However, as observed by [1], the main limitation of all the active contour methods presented so far, is that the appearance of the B-mode image depends on the characteristic of the IVUS system and the parameters used for the image reconstruction. Thus, no segmentation method is guaranteed to perform correctly on IVUS images from different systems. A third strategy was explored by Kudo [8], who observed that during successive frames of the IVUS sequence, the texture inside the lumen exhibits a large variability of the speckle pattern due to the presence of blood flow, while the speckle pattern changes slowly in the tissue area. Kudo [8] introduced a model-based approach, exploiting the decorrelation generated by the blood flow. The feasibility of the approach [8] was illustrated by an *in vitro* experiment, using an acrylic tube phantom. Unfortunately the method cannot be straightforwardly extended to *in vivo* images because the model didn't account for the vessel pulsations and catheter oscillations. We decided, for the first time, to extend his approach by building a workflow applied to *in vivo* sequences.

In this paper we propose to first identify the most stable frames of the pullback, then register its contiguous frames in order to generate a parametric image discriminating the presence of steady tissues from the blood and finally segments the vessel lumen by classifying the vessel pixels. The method automatically segments the lumen border by combining temporal information obtained computing the local correlation between successive frames of the sequence with spatial classification performed using the Growcut [9] algorithm.

The main advantage of this approach is the segmentation robustness due to the combination of temporal and spatial analysis.

2 Method

The proposed segmentation method is composed of two steps: a model-based temporal correlation analysis and a spatial classification. The pipeline of the approach is sketched in Fig 2-a.

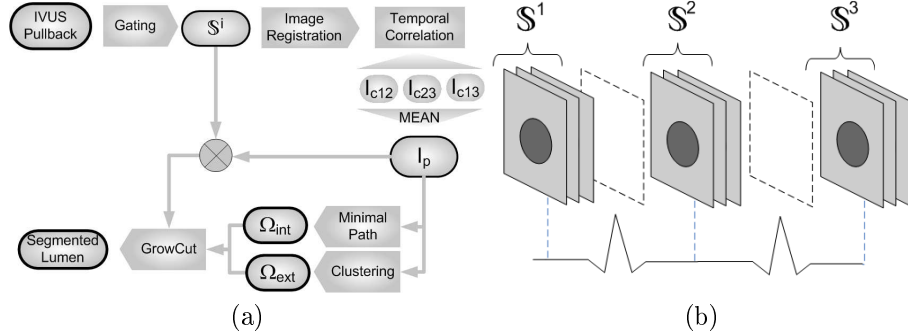


Fig. 2. Pipeline of the lumen segmentation method (a) and frames selection scheme (b).

2.1 Model-based temporal analysis

Frames selection and motion compensation Heart beating causes a repetitive longitudinal oscillation of the catheter (swinging effect) along the vessel axis, resulting in multiple sampling of the same vessel positions. Additionally the best alignment between vessel tissues can be achieved when the arterial pulsation is minimal. For this reasons the the most stable frames of the pullback, commonly interpreted as belonging to the end-diastolic phase, can be robustly identified by ECG gating or, as in our case, by image-based gating [10]. Then, in order to take advantage of the information present in successive frames of the pullback, for each gated frame $I^G = I(x, y; G)$ (where G is a gated frame index), the previous and successive frames of the pullback are extracted for composing a local stack $S^i = \{I^{G-1}, I^G, I^{G+1}\}$. Figure 2-b summarizes the frame selection process and the creation of local stacks. Finally, possible catheter translation and rotation, due to in-plane oscillation are compensated by computing a registration between all the stack frames. The optimal rigid registration is obtained by computing the transformation parameters that minimizes the mutual information between two successive according to the equation $X_2 = R(\theta) \cdot X_1 + T$ where $X = \begin{bmatrix} x \\ y \end{bmatrix}$, $R(\theta)$ is the rotation matrix, and T is the translation matrix.

Temporal correlation As proposed by [8], the correlation between successive frames of an IVUS sequence can provide useful information for the lumen border detection. In order to compute the temporal correlation of the speckle pattern as discriminative feature, the Pearson Correlation Coefficient is computed over a sliding window of size $H \times H$ along each pair of images of a stack S^i generating three correlation images ($I_{c12}, I_{c23}, I_{c13}$). The size of the window H is a trade off between edge over-smoothing when large windows are used and lack

of precision in the correlation computation when a small number of samples are involved. The optimal size can be defined as the distance between two speckle noise peaks which can be automatically obtained from the duration of the pulse waveform [11], computed as the *full width at half maximum* of the noisy auto-correlation coefficient. Finally a parametric image I_P is computed by averaging the correlations ($I_{c12}, I_{c23}, I_{c13}$) (Figure 3-a).

2.2 Spatial classification

In this paper a fast and robust spatial segmentation technique has been used to classify the image pixel. The Growcut algorithm [9] is an iterative classification method assuring the spatial coherence of the segmentation. The method is able to optimally separate two regions of an image, R_A and R_B according to the pixel spatial relations and intensity. The approach relies to a cellular automaton technique, discrete in both space and time, that operates on pixels p of the image I and its neighborhood cells p . A cellular automaton system, is based on a cell state defined by a triplet $\Gamma = (L_p, \theta_p, V_p)$, where L_p is the label of the current cell, θ_p is the weight of the current cell, and V_p is the textural feature (in our case the intensity of the gray-scale image). The seeded cells are initially defined by labeling two compact subsets of the image (Ω_A and Ω_B) composed by all the pixel who likely belong to the external and internal regions R_A and R_B respectively, while not-assigned pixels Ω_C are initially set to: $L_p = 0$ and $\theta_p = 0$. The cell's state Γ_q^{t+1} at time step is defined by a rule considering the states of the neighborhood cells Γ_q^t at previous time step t . Starting from the initial seeds, at each iteration, the strongest neighbor cells q propagate its label to the cell p , and the new strengths of θ_p is computed weighting the strength of the neighbor cell and its distance:

$$\theta_p^{t+1} = g(\|V_p - V_q\|) \theta_q^{t+1} \quad (1)$$

where $\| \cdot \|$ is the euclidean distance and g is a monotonically decreasing function defined as $g(\xi) = 1 - \frac{\xi}{\max(V)}$. The final goal of the segmentation is to assign a label to all the pixels.

Labels The initial Growcut seed areas, Ω_A and Ω_B , are computed from the polar parametric image I_P , which is characterized by low correlation where the blood is flowing (lumen area) and high correlation where the arterial vessel and plaque are present. The correlation reaches its maximum close to the lumen border, and progressively decrease with the dept of the signal.

Based on these assumptions, the contour of Ω_A (Fig 3), corresponding to the surrounding tissues, is obtained by identifying the maximum intensity profile along the columns of I_P . The tracking of the ridge is done by the minimum cost path technique proposed by Cohen [12]. Such method computes the contour guaranteeing the minimal trajectory along an energy potential surface between two end points. The potential surface depends on both intensity of the image and distance from the target point. The method provides a smooth curve able

to connect tissues separated by discontinuities (for instance generated by the shadow of the catheter guide, by stent wires or by calcium spots). The minimal path method [12] requires the definition of source and target coordinates. These are obtained as the image coordinate of the maximum intensity computed on the first and the last column of the image.

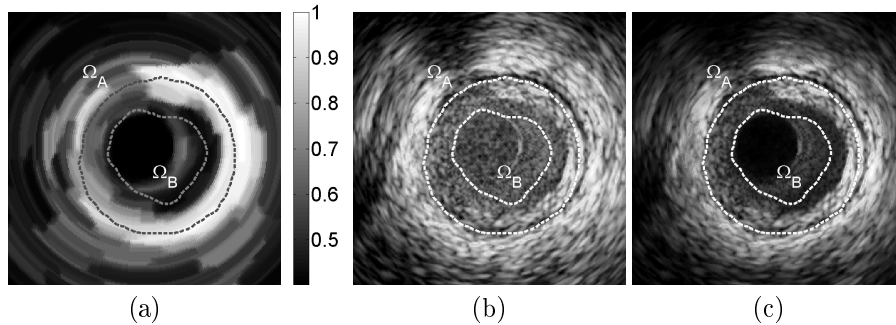


Fig. 3. Growcut seed areas Ω_A and Ω_B superimposed to the parametric image I_P (a) to the initial frame I^G (b) and to the modulated frame I_P^G (c).

The second contour Ω_B , corresponding to the blood area is obtained by classifying the pixel of the polar parametric image I_P enclosed in Ω_A . Such samples can be either blood vessel or surrounding tissues, hence the pixels having low correlation are identified applying the classical Otsu threshold method [13] to the pixels enclosed in Ω_B .

Modulated images The Growcut classification method is applied to the modulated image I_M^G obtained multiplying the gated frame I^G for the parametric image I_P^G . Such modulation combines the high frequencies of the IVUS image I^G , with the low frequencies of the parametric map I_P^G . Hence, it enhances the boundaries between lumen and plaque (especially in the regions where the speckle echogenicity is similar), since in I_P , the vessel border is sharp and lumen and vessel areas are uniform. Figure 3 illustrate the Growcut seed areas Ω_A and Ω_B superimposed to the parametric image I_P to the initial frame I^G and to the modulated frame I_M^G .

3 *In vivo* experiments

The proposed segmentation method has been tested on three pullbacks, (each of them composed by about 2000 frames, for a total of 300 gated frames) of *in vivo* coronary images. Such database guarantees a representative number of different vascular structures (plaque and vessel shape, presence of stent, different lumen area and diameter). The acquisition has been performed using an IVUS Galaxy II System with a catheter Atlantis SR Pro 40 MHz (Boston Scientific).

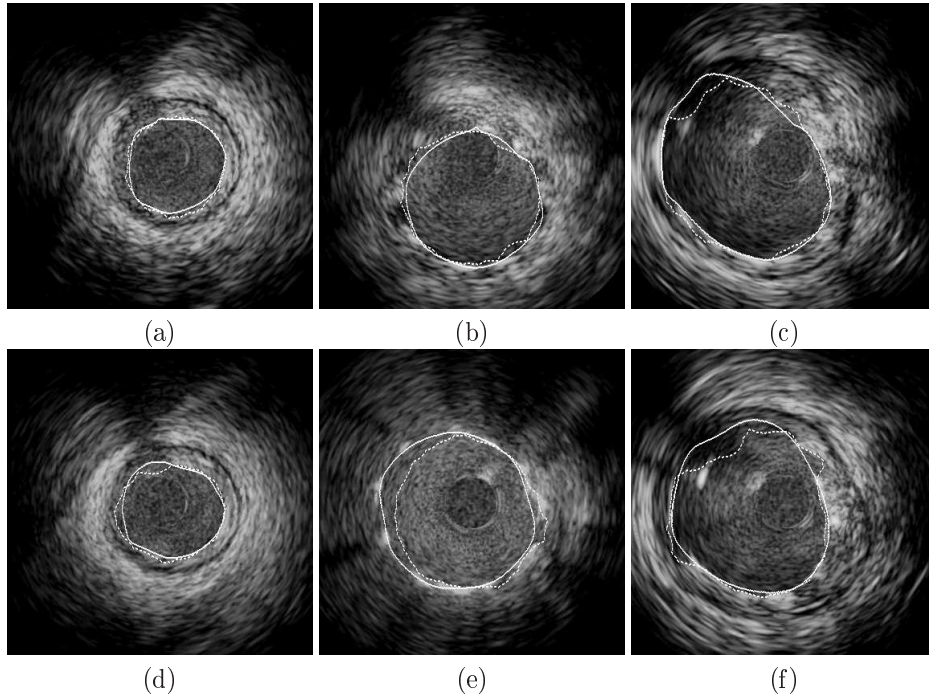


Fig. 4. Examples of segmented images (vessel (a-d), stent (b-e) and bifurcation (c-f) frames). The continuous and dotted lines represent respectively the manual and the automatic contours.

Ground truth areas, indicating the expected segmentation result, were manually delineated in each gated frames of the IVUS pullback by two experts. In order to obtain a fairly segmented reference data set, the validation interface enabled the expert to navigate from the previous/successive frame to provide insights about the temporal evolution of the pullback. The operator performing the analysis was blinded to the automatic and to the other manual segmentation results. Figure 4 illustrates some segmentation examples of general vessel, stent and bifurcation frames, respectively first, second and third column obtained using a window size of $0.56 \times 0.56 \text{ mm}^2$. In the first row three successfully segmented frames are shown. In particular Figure 4-a illustrates how the segmentation of a challenging frame, in which only half of the plaque contour is visible (see Figure 1), has been achieved. The second row of Figure 4 present cases in which the result is not optimal. In Figure 4-d and -f the algorithm is fooled by the catheter guide, while in Figure 4-e the segmentation under-estimates the temporal correlation lumen area.

Table 1. Segmentation errors in [mm] computed as the distance between automatic and manual observers contours

	Automatic		Inter-observer	
	Max	Mean	Max	Mean
Vessel	0.57 ± 0.24 [mm]	0.17 ± 0.08 [mm]	0.59 ± 0.73 [mm]	0.16 ± 0.06 [mm]
Stent	0.62 ± 0.19 [mm]	0.18 ± 0.07 [mm]	0.54 ± 0.31 [mm]	0.15 ± 0.06 [mm]
Bifurcation	1.12 ± 0.44 [mm]	0.31 ± 0.12 [mm]	1.80 ± 2.57 [mm]	0.23 ± 0.11 [mm]

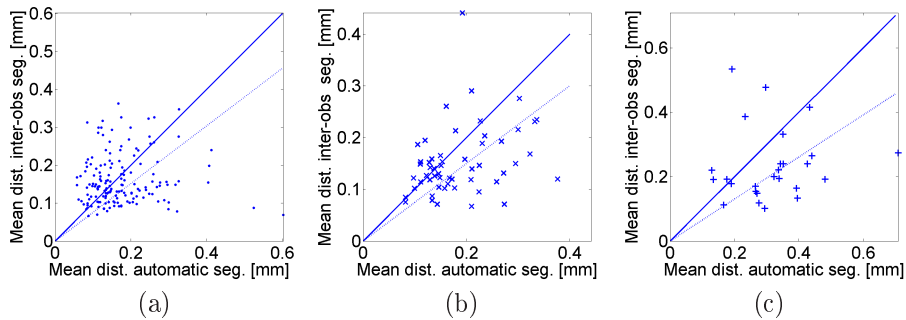


Fig. 5. Scatter plots comparing the automatic with the inter-observer segmentation errors. The plots report the average error measurements in the case of a vessel (a), stent (b), and bifurcation (c) frames. The solid and the dotted lines represent the unitary slope line and the linear regression curve, respectively.

4 Discussion

In this paper we presented a lumen segmentation method which combines temporal information extracted from successive frames of the sequence with spatial classification issues from the spatial analysis. Encouraging results has been obtained, since the automatic and manual segmentation error are similar in most of the cases. The performance of the approach is particularly good in vessel and stent frames showing an average segmentation error of 0.17 ± 0.08 mm and 0.18 ± 0.07 mm respectively. This approach is fully automatic and additionally it doesn't require parameter tuning or training making it potentially suitable for segmenting images from different echographs.

Future work will be addressed towards the validation of the technique comparing the performance on pullbacks belonging to different echographs brands, models and probes (different central frequency). The proposed framework will be evaluated using alternative spatial segmentation methods such as GraphCut algorithm. Finally, the applicability of the method to the whole pullback sequence is in progress.

Acknowledgments

This paper has been partially supported by projects TIN2009-14404-C02, La Marató de TV3 082131 and CONSOLIDER-INGENIO CSD 2007-00018. E-mail: balocco.simone@gmail.com.

References

1. E. G. Mendizabal-Ruiz, G. Biros, and I. A. Kakadiaris, "An inverse scattering algorithm for the segmentation of the luminal border on intravascular ultrasound data," *Med Image Comput Comput Assist Interv*, vol. 12, no. Pt 2, pp. 885–92, 2009.
2. G. Unal, S. Bucher, S. Carlier, G. Slabaugh, T. Fang, and K. Tanaka, "Shape-driven segmentation of the arterial wall in intravascular ultrasound images," *IEEE Trans Inf Technol Biomed*, vol. 12, no. 3, pp. 335–47, may 2008.
3. D. Gil, P. Radeva, J. Saludes, and J. Mauri, "Automatic segmentation of artery wall in coronary ivus images: a probabilistic approach," *Comput Cardiol*, pp. 687–690, 2000.
4. E. Brusseau, C. D. Korte, F. Mastik, J. Schaar, and A. V. D. Steen, "Fully automatic contour detection in intravascular ultrasound imaging," *IEEE Trans Med Imag*, vol. 5, no. 27, pp. 108–118, 2004.
5. J. D. Klingensmith, R. Shekhar, and D. G. Vince, "Evaluation of three-dimensional segmentation algorithms for the identification of luminal and medial-adventitial borders in intravascular ultrasound images," *IEEE Trans Med Imaging*, vol. 19, no. 10, pp. 996–1011, Oct 2000.
6. H. Jianming and H. Xiheng, "An approach to automatic segmentation of 3d intravascular ultrasound images," in *Nuclear Science Symposium and Medical Imaging Conference*, vol. 3, 1994, pp. 1461–1464.
7. M. Sonka, W. Liang, X. Zhang, S. DeJong, S. M. Collins, and C. R. McKay, "Three-dimensional automated segmentation of coronary wall and plaque from intravascular ultrasound pullback sequences," *Computers in Cardiology 1995*, pp. 637–640, 1995.
8. N. Kudo, T. Kanenari, X. Zhang, and K. Yamamoto, "In vitro study on arterial lumen detection using a correlation technique in ivus," vol. 2, 1998, pp. 830–831.
9. V. Vezhnevets and V. Konouchine, "Grow-cut" - interactive multi-label n-d image segmentation," 2005, pp. 150–156.
10. C. Gatta, S. Balocco, F. Ciompi, R. Hemetsberger, O. R. Leor, and P. Radeva, "Real-time gating of ivus sequences based on motion blur analysis: Method and quantitative validation." *Med Image Comput Comput Assist Interv*, vol. 13, pp. 59–67, 2010.
11. S. F. Smith and R. F. Wagner, "Ultrasound speckle size and lesion signal to noise ratio: verification of theory," *Ultrason Imaging.*, vol. 6, no. 2, pp. 174–80, 1984.
12. L. Cohen and R. Kimmel, "Global minimum for active contour models: A minimal path approach," *International Journal of Computer Vision*, vol. 24, pp. 57–78, 1997.
13. N. Otsu, "A threshold selection method from gray-level histograms," *IEEE Transactions on Systems, Man and Cybernetics*, vol. 9, no. 1, pp. 62–66, 1979.